Science Discovery Physics
2026, Vol. 1, No. 1, pp. 70–87
https://doi.org/10.11648/j.sdp.20260101.17

Research Article

Impact of Albedo, Heterogeneity, Perturbations and Circumstellar Dust in the Circular Restricted Three-body Problem

Jagadish Singh[1], **Sunusi Haruna**[2, *]

[1]Department of Mathematics, Ahmadu Bello University, Zaria, Nigeria

[2]Department of Science and Engineering, Kano State Polytechnic, Kano, Nigeria

Abstract

This paper explore the dynamical influence of multiple astrophysical motivated perturbations in the framework of the circular restricted three-body problem (CR3BP), focusing on the stability and evolution of trajectories near the triangular libration points. The model incorporates albedo-related radiation pressure, mass heterogeneity of the primaries, additional perturbing forces, and the gravitational potential from a circumstellar dust belt, simulating a more realistic environment such as that found in binary stellar systems surrounded by debris disks. By extending the classical CR3BP to include these effects, we investigate their combined impact on the topology of the phase space, the location and stability of the libration points. Numerical simulations reveal that circumstellar dust and reflective radiation can significantly deform the effective potential landscape, leading to shifts in equilibrium locations and the emergence of new dynamical behaviours. The findings provide insight into the complex dynamical environments of young stellar binaries, protoplanetary systems, and dust-rich exoplanetary configurations, and may inform future observational or mission-planning efforts in such contexts. Besides the three collinear libration points typically seen in classical models, the effects of heterogeneity and the belt introduce an additional collinear point, though it is linearly unstable. The findings of this study could be applied to the motion of celestial bodies under the influence of perturbing forces such as heterogeneity, the Albedo effect, and the belt.

Keywords

CR3BP, Perturbation, Albedo, Heterogeneous Spheroid, Potential from a Belt

1. Introduction

Circular restricted three-body problem (CR3BP) defines the motion of an infinitesimal body in the gravitational field of two bodies called primaries that move in circular orbits about their centre of mass in a plane. CR3BP possess five equilibrium points, which three are collinear points L_1, L_2 and L_3 whose line join the primaries and the two triangular points L_4 and L_5 formed the equilateral triangles with the primaries making five co-planar equilibrium points (Singh and Ishwar [17], Singh and Raheem [1], Singh and Haruna [12]) investigated the stability of equilibrium points under the

*Correspondence: Sunusi Haruna (siyudiso@gmail.com)

Received: 12 April 2025; **Accepted:** 4 May 2025; **Published:** 12 March 2026

influence of small perturbation in the Coriolis and centrifugal force together with effects of oblateness of three primaries and both are radiating. It has found that non-collinear points are stable for $0 \le \mu < \mu_c$ and unstable for $\mu_c \le \mu < \frac{1}{2}$ where μ_c is the critical mass parameter which depend on the perturbations, while collinear points remain unstable. Important research in R3BP in respect of libration points of photo gravitation, the primary is source of radiation and oblate spheroid is the bigger by Sharma in 1982. He found that in the linear sense there exist a collinear retrograde elliptical periodic orbits around the triangular points and in the case of the mass parameter, the triangular points have long and short-periodic retrograde elliptical orbits which resulted to increase in oblateness and radiation force when the value of the critical mass is reduces. Suraj et al. Studied Stability of equilibrium points in R3BP under influence of luminous and heterogeneous spheroid primaries with three layers of different density was studied, the result showed, the position of the non-collinear points and its stability found that due to the influence of the participated perturbations moves a way slightly from the line joining the primaries. The stability found when $0 \le \mu < \mu_c$ where it reduces the range due the perturbations, while the collinear points remain unstable [10]. Kumari et al investigated the non-linear stability of the triangular point L_4 in R3BP when the smaller primary is heterogeneous spheroid with three layers having different densities, is stable in the range of $0 < \mu < \mu_c$ [9] Recently Kumari et al. examined the stability in R3BP under effect of when the smaller primary heterogeneous spheroid with three layers having different densities while the bigger primary is considered as a point mass, they found three collinear points and two triangular points. The collinear points are unstable while the triangular points are conditionally stable for the mass parameter $\mu \in (0, \mu_c)$, where $\mu_c = 0.5856 k_1$ [8].

Albedo is commonly applied to the overall average reflection coefficient of an object as dimensionless quantity and non-gravitational force that exists valuable effect on the movement of masses and their stability.

Albedo is an expression of ability of a surface to reflect sunlight (heat from Sun), a light colour surface returns (reflect) a large part of the sun rays back to the atmosphere with high Albedo of 1, while the dark surface absorb the rays from the Sun with low Albedo of 0. Since there are no dark-body planets in our solar system.

A study of momentum of the celestial bodies in the dynamical system and their stability has meaningful impact, this had inspired many researchers to studied its effects in the R3BP, they found three collinear points and two triangular points. The collinear points are unstable while the triangular are stable as well as their stability equally respectively (Shipra et al [11], Idrisi and ullah [6], Idrisi, M. J. [3, 4], Idrisi and ullah, [5]).

Singh J. and Tyokyaa, K.. Studied the effects of Albedo in the ER3BP with an oblate primary, a triaxial secondary, and potential due to belt for the Earth-Moon system, the found that, as the parameter above increases or decreases resulted to shift the triangular position L_4 and L_5 toward the center of the origin and away from the center of the origin respectively. Both the position and stability of the triangular points is conditionally stable as $0 \le \mu < \mu_c$ for stable libration points and $\mu_c \le \mu \le \frac{1}{2}$ for unstable libration points [16].

The motion around triangular points in CR3BP with radiating, heterogeneous primaries, surrounded by a belt was examined by Singh and Haruna, they found the stability of the non-collinear points is stable while the collinear points are unstable but there are additional collinear points due to the influenced of the belt in some cases [13].

Ansari et al studied the CR3BP; they located all the equilibrium for in-plane and out of plane equilibrium point and found that, they are unstable [2].

Recently Kumari et al. examined the stability in the R3BP under the effect of heterogeneous spheroid, where the smaller primary is a heterogeneous spheroid with three layers having different densities while the bigger primary is consider as point mass, they found three collinear and two non-collinear points, the collinear points are unstable while non-collinear points are conditionally stable for the mass parameter $\mu \in (0, \mu_c), \mu_c = 0.585688 K_1$ [8].

Dust rings surrounding the binary stars had inspired many scientists to study the CR3BP by taking into account the additional gravitational potential from the belt.

The belt however, Jiang and Yeh in their studied in CR3BP found that, the influence from the ring-type circular cluster of material points makes the structure of the dynamical system quite different so that new libration point exist under certain condition [7].

Singh and Taura (investigated the motion of an infinitesimal body in the generalized restricted three-body problem. Their problem was generalized in the sense that both primaries are radiating, oblate bodies, together with the effect of gravitational potential from a belt. The equations of motion were derived and the positions of the equilibrium points were found and it was seen that in addition to the usual five equilibrium points, two new collinear points were discovered due to the potential from the belt. The linear stability analysis of the equilibrium points show that collinear equilibrium points remain unstable, while the triangular points are stable under some conditions influenced by the oblateness, radiation of the primaries and potential from the belt [14].

In an investigation by Singh and Taura the effect of the triaxiality of the more massive primary, oblateness of the less massive primary and the infinitesimal body and the gravitational potential from the belt on the location of $L_{4,5}$ and their linear stability in CR3BP, they found that, the range of the stability of the triangular points from $0 < \mu < \mu_c$ increases due to the potential from the belt [15].

Recently, Singh and Tyokyaa studied Albedo effect in ER3BP with an oblate primary, a triaxial secondary and potential due to a belt, they found that with the increase of the parameters leads the position of $L_{4,5}$ away from the center of the origin and made the range unstable [16].

In this paper, effect of Albedo, Heterogeneity, Perturbation and Circumstellar dust in the CR3BP for the Earth-Moon system are studied.

The paper is organized in six sections; the introduction is given in this section. The next section describes the equations of motions, the position of the equilibrium points are studied in sect. 3. While their stability is discussed in sect. 4. Numerical illustration are given in section 5. Then the discussion and conclusion are drawn in sect. 6.

Following the works of Suraj et al. [10] and Singh and Taura [19], studied the locations of collinear and triangular libration points and their linear stability, For numerical applications, the Earth-Moon system is utilized.

2. Equations of Motion

Using dimensionless variables and adopting a barycentric rotating system about z-axis with constant angular velocity, the equations of motion of the infinitesimal mass under the influences of albedo, heterogeneity, perturbations and circumstellar dust can be expressed as;

$$\ddot{x} - 2n\alpha\dot{y} = \Omega_x$$
$$\ddot{y} + 2n\alpha\dot{x} = \Omega_y$$

with force function as follows.

$$\Omega = \frac{n^2\beta}{2}\left(x^2+y^2\right) + A_E\left(\frac{1-\mu}{r_1} + \frac{k_1}{2r_1^3}\right) + A_M\left(\frac{\mu}{r_2} + \frac{k_2}{2r_2^3}\right) + \frac{M_b}{\left(r^2+T^2\right)^{\frac{1}{2}}} \tag{1}$$

$$0 < \mu = \frac{m_2}{m_1+m_2} \le \frac{1}{2}, m_1 > m_2 >> m_3$$

$$r_1^2 = \left(x-\mu\right)^2 + y^2, r_2^2 = \left(x-\mu+1\right)^2 + y^2, r^2 = x^2 + y^2,$$

$$n^2 = 1 + \frac{3}{2}k_3 + \frac{2M_b r_c}{\left(r_c^2+T^2\right)^{\frac{3}{2}}} \tag{2}$$

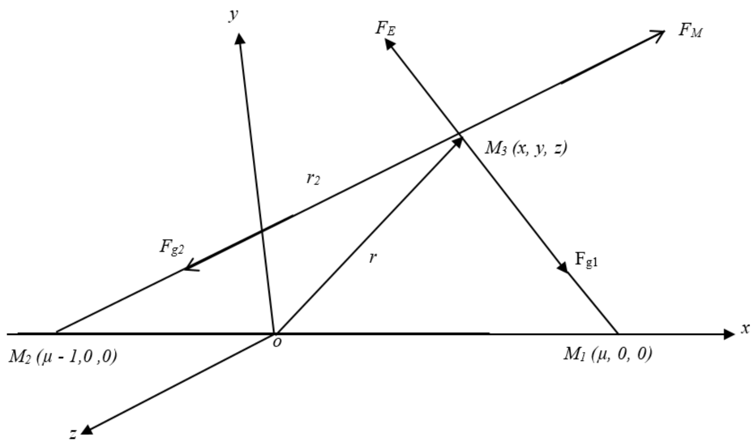

Figure 1. Configuration of CR3BP under Albedo effect, Heterogeneous primaries and a Belt.

From the above figure, M_1 and M_2 are the primaries, with masses $m_1 > m_2$. Then M_3 is the infinitesimal body with negligible mass $m_3 << m_2$. r_1, r_2 and r are respective distances of M_3 from M_1, M_2 and the barycenter 0. More so, F_{g1} and F_{g2} are the gravitational forces acting on M_3 due to M_1 and M_2 respectively. F_E and F_M are the albedo force acting on M_3 due to the solar radiation reflected by M_1 and M_2 respectively.

Now, the forces acting on M_3 due to M_1 and M_2 are

$F_{g1}\left(1-\frac{F_E}{F_{g1}}\right)=F_{g1}(1-\propto_E)$ and $F_{g2}\left(1-\frac{F_M}{F_{g2}}\right)=F_{g2}(1-\propto_M)$ respectively. Then $\propto_E=\frac{F_E}{F_{g1}}<<1$ and $\propto_M=\frac{F_M}{F_{g2}}<<1$. Thus A_E and A_M are Albedo factors such that $A_E=1-\propto_E$, and $A_M=1-\propto_M$. Also, $\propto_E$ and $\propto_M$ can be expressed as; $\propto_E=\frac{l_1}{2\pi G m_1 C\sigma}$; $\propto_M=\frac{l_2}{2\pi G m_2 C\sigma}$ where l_1 and l_2 are the luminosity of the bigger and the smaller primary respectively, G is the gravitational constant, c is the speed of light and σ is mass per unit area of the infinitesimal mass M_3. Now, $\frac{\propto_M}{\propto_E}=\frac{m_1 l_2}{m_2 l_1}$ *that is*, $\propto_M=\propto_E\left(\frac{1-\mu}{\mu}\right)h$, where $m_1=(1-\mu), m_2=\mu$. $h=\frac{l_2}{l_1}=constant$.

$k_i(i=1,2,3)$ are parameters for being heterogeneous primaries with three layers of different densities. μ is the mass parameter, n is the mean motion of the primaries; $\alpha=1+\varepsilon, \varepsilon<<1$, $\beta=1+\varepsilon', \varepsilon'<<1$ are the parameters for the Coriolis and centrifugal forces respectively, to which small perturbations ε and ε' are given. M_b is the total mass of the belt. $T=a+b$, where a and b are parameters which determine the density profile of the belt.

Zero Velocity Curves (ZVC) / Surface

The system (1) is difficult to interpret the motion of the infinitesimal body, therefore zero velocity curves (ZVC) give ability to identify regions where particle can have either bound or unbound orbits relative to the two massive bodies in the (x-y) plane when the numerical value of the Jacobian constant C is obtained using initial values in the equation

$$2\Omega-\left(\dot{x}^2+\dot{y}^2+\dot{z}^2\right)=C. \quad (3)$$

The zero velocity curves and zero velocity surfaces are presented in the following figures.

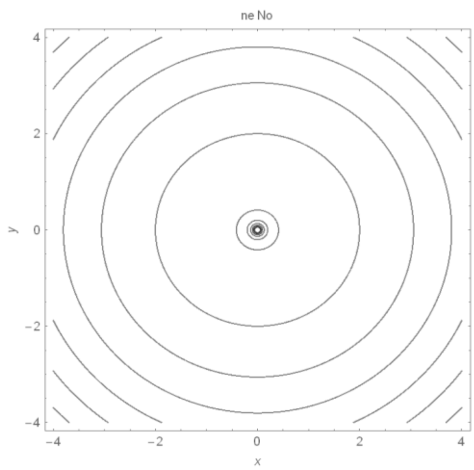

Figure 2. *The zero velocity curves for the Earth-Moon system in (2-D) for* $\mu=0.215, A_E=A_M=1, k_i(i=1,2,3)=0, M_b=0.00, \varepsilon'=0.00$

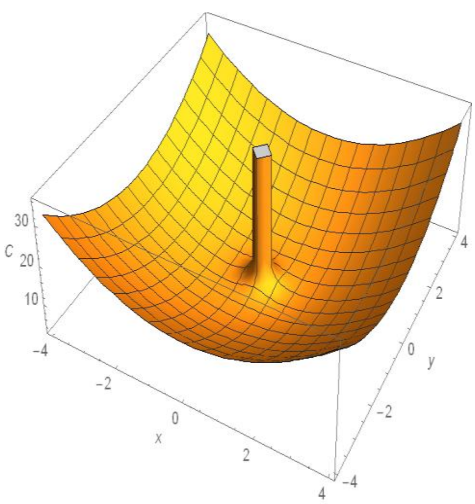

Figure 3. *The zero velocity surfaces for the Earth-Moon system in (3-D) for* $\mu=0.215, A_E=A_M=1, k_i(i=1,2,3)=0, M_b=0.00, \varepsilon'=0.00$.

3. Locations of the Equilibrium Points

The equilibrium points are the solution of the dynamical system (1) where the infinitesimal mass is at rest i.e., $\dot{x} = \dot{y} = \ddot{x} = \ddot{y} = \ddot{z} = 0$ in system (1) yield

$$\Omega_x = n^2\beta x - \frac{(1-\mu)(x-\mu)A_E}{r_1^3} - \frac{3(x-\mu)k_1A_E}{2r_1^5} - \frac{\mu(x-\mu+1)A_M}{r_2^3} - \frac{3(x-\mu+1)k_2A_M}{2r_2^5} - \frac{M_b x}{\left(r^2+T^2\right)^{\frac{3}{2}}} = 0$$

$$\Omega_y = y\left[n^2\beta - \frac{(1-\mu)A_E}{r_1^3} - \frac{3k_1A_E}{2r_1^5} - \frac{\mu A_M}{r_2^3} - \frac{3k_2A_M}{2r_2^5} - \frac{M_b}{\left(r^2+T^2\right)^{\frac{3}{2}}}\right] = 0 \tag{4}$$

The last equation indicates that either the expression in the bracket is zero or y = 0.

3.1. Triangular Points

The triangular equilibrium points can be obtained by solving $\Omega_x = \Omega_y = 0$, when $y \neq 0$

Re-writing the first equation of (4), we have

$$\begin{aligned} &x\left[n^2\beta - \frac{A_E(1-\mu)}{r_1^3} - \frac{3k_1A_E}{2r_1^5} - \frac{\mu A_M}{r_2^3} - \frac{3k_2A_M}{2r_2^5} - \frac{M_b}{\left(r^2+T^2\right)^{\frac{3}{2}}}\right] + \frac{A_E\mu(1-\mu)}{r_1^3} + \frac{3\mu k_1A_E}{2r_1^5} + \\ &+ \frac{\mu^2A_M}{r_2^3} - \frac{\mu A_M}{r_2^3} + \frac{3\mu k_2A_M}{2r_2^5} - \frac{3k_2A_M}{2r_2^5} = 0 \end{aligned} \tag{5}$$

and in the case $y \neq 0$, the second equation becomes

$$n^2\beta - \frac{A_E(1-\mu)}{r_1^3} - \frac{3k_1A_E}{2r_1^5} - \frac{\mu A_M}{r_2^3} - \frac{3k_2A_M}{2r_2^5} - \frac{M_b}{\left(r^2+T^2\right)^{\frac{3}{2}}} = 0 \tag{6}$$

The triangular points are the solutions of eqs. (5) and (6) when $y \neq 0$. Therefore, we get

$$(1-\mu)\left[n^2\beta - \frac{A_E}{r_1^3} - \frac{M_b}{\left(r^2+T^2\right)^{\frac{3}{2}}}\right] = \frac{3k_1A_E}{2r_1^5} \tag{7}$$

$$\mu\left[n^2\beta - \frac{A_M}{r_2^3} - \frac{M_b}{\left(r^2+T^2\right)^{\frac{3}{2}}}\right] = \frac{3k_2A_M}{2r_2^5} \tag{8}$$

If the primaries are neither heterogeneous nor suffering from the effects of Albedo and the belt, then $k_i(i=1,2,3)=0, M_b=0, A_E \; \& \; A_M = 1, n=1$, and eqs. (7) and (8) reduce to

$$r_1^3 = r_2^3 = \frac{1}{\beta}, \tag{9}$$

Now we assume that, there is Albedo effect and heterogeneity of the primaries and the potential from the belt are also present, then the r_1 and r_2 will take the form,

$$\begin{aligned} r_1 &= \frac{1}{\beta^{\frac{1}{3}}} + \varepsilon_1 \\ r_2 &= \frac{1}{\beta^{\frac{1}{3}}} + \varepsilon_2 \end{aligned} \tag{10}$$

where $|\varepsilon_i| << 1$, for i = 1, 2.

Substituting the values of $r_i(i=1,2)$ and n from (2) and

(10) in (7) and (8) respectively and putting $\beta = 1+\varepsilon'$, $A_M = 1-\alpha_M$, $A_E = 1-\alpha_E$, $|\alpha_M| << 1$, $|\alpha_E| << 1$ and restricting to the linear terms in $\varepsilon_i, k_i, \alpha_E, \alpha_M, \varepsilon'$ and M_b, we obtain

$$\varepsilon_1 = \frac{k_1}{2(1-\mu)} - \frac{k_3}{2} - \frac{\alpha_E}{3} - \frac{M_b(2r_c-1)}{3(r_c^2+T^2)^{\frac{3}{2}}}$$

$$\varepsilon_2 = \frac{k_2}{2\mu} - \frac{k_3}{2} - \frac{\alpha_M}{3} - \frac{M_b(2r_c-1)}{3(r_c^2+T^2)^{\frac{3}{2}}} \tag{11}$$

Substituting these values in equations (10) we have

$$r_1 = \frac{1}{\beta^{\frac{1}{3}}} - \frac{k_1}{2(1-\mu)} - \frac{k_3}{2} - \frac{\alpha_E}{3} - \frac{M_b(2r_c-1)}{3(r_c^2+T^2)^{\frac{3}{2}}}$$

$$r_2 = \frac{1}{\beta^{\frac{1}{3}}} + \frac{k_2}{2\mu} - \frac{k_3}{2} - \frac{\alpha_M}{3} - \frac{M_b(2r_c-1)}{3(r_c^2+T^2)^{\frac{3}{2}}} \tag{12}$$

Substituting equations (12) in (2) and solving, we get

$$x = \mu - \frac{1}{2} + \frac{1}{2}\left(\frac{k_2}{\mu} - \frac{k_1}{(1-\mu)}\right) + \frac{1}{3}(\alpha_E - \alpha_M)$$

$$y = \pm\frac{\sqrt{3}}{2}\left[1 - \frac{4}{9}\varepsilon' + \frac{k_1}{3(1-\mu)} + \frac{k_2}{3\mu} - \frac{2k_3}{3} - \frac{2\alpha_E}{9} - \frac{2\alpha_M}{9} - \frac{4M_b(2r_c-1)}{9(r_c^2+T^2)^{\frac{3}{2}}}\right] \tag{13}$$

Equation (13) is the location of the triangular libration points of the problem under study.

3.2. Location of Collinear libration Points

The collinear equilibrium points are solutions of the equations (4) with $y=0$. Then it yields.

$$n^2\beta x - \frac{(1-\mu)(x-\mu)A_E}{r_1^3} - \frac{3(x-\mu)k_1A_E}{2r_1^5} - \frac{\mu(x-\mu+1)A_M}{r_2^3} - \frac{3(x-\mu+1)k_2A_M}{2r_2^5} - \frac{M_b x}{(x^2+T^2)^{\frac{3}{2}}} = 0$$

with

$$r_1 = |x-\mu| \;,\; r_2 = |x-\mu+1| \tag{14}$$

denoting the left side of eq. (14) by $f(x)$,

$$f(x) = n^2\beta x - \frac{(1-\mu)(x-\mu)A_E}{r_1^3} - \frac{3(x-\mu)k_1A_E}{2r_1^5} - \frac{\mu(x-\mu+1)A_M}{r_2^3} - \frac{3(x-\mu+1)k_2A_M}{2r_2^5} - \frac{M_b x}{(x^2+T^2)^{\frac{3}{2}}} \tag{15}$$

Now we observed that,

$$\frac{df(x)}{dx} = n^2\beta + \frac{2A_E(1-\mu)}{|x-\mu|^3} + \frac{6k_1A_E}{|x-\mu|^5} + \frac{2\mu A_M}{|x-\mu+1|^3} + \frac{6k_2A_M}{|x-\mu+1|^5} + \frac{3M_bx^2}{(x^2+T^2)^{\frac{5}{2}}} - \frac{M_bx}{(x^2+T^2)^{\frac{3}{2}}} \tag{16}$$

And so

$\frac{df(x)}{dx} > 0$, if

$$n^2\beta + \frac{2A_E(1-\mu)}{|x-\mu|^3} + \frac{6k_1A_E}{|x-\mu|^5} + \frac{2\mu A_M}{|x-\mu+1|^3} + \frac{6k_2A_M}{|x-\mu+1|^5} + \frac{3M_bx^2}{(x^2+T^2)^{\frac{5}{2}}} > \frac{M_bx}{(x^2+T^2)^{\frac{3}{2}}}$$

Therefore, when $x = \pm\infty$, we have $\frac{df(x)}{dx} = n^2\beta$

When $x = \mu - 1$, eq. (16) gives $\frac{df(x)}{dx} = \infty$

When $x = \mu$, equation (16) gives $\frac{df(x)}{dx} = \infty$

Now from eq. (15), when $x = \mu - 2$, we observed that $f(\mu-2) < 0$, for $\beta \approx 1, M_b << 1, k_i, i = 1,2$ and $\alpha_{E,}\alpha_M \approx 1$

When $x = 0$, we found that $f(0) > 0$, while for $x = \mu + 1$, $f(\mu+1) > 0$

Therefore, the real roots of the equation (14) will lie in the open intervals $(\mu-2, \mu-1), (\mu-1, 0)$ and $(\mu, \mu+1)$. these roots correspond to the collinear points $L_i, i = 1,2,3$ we donate them appropriate when they are found.

Now, to locate the collinear points we divide the orbital plane into following three parts:

$-\infty < x < \mu-1,\quad \mu-1 < x < \mu,\quad \mu < x < \infty,$

with respect to the primaries,

Case 1: Location of $L_1(x < \mu-1)$

Let the collinear point L_1 be on the left side of the smaller primary at a distance ε_1 from it on the x-axis. Then

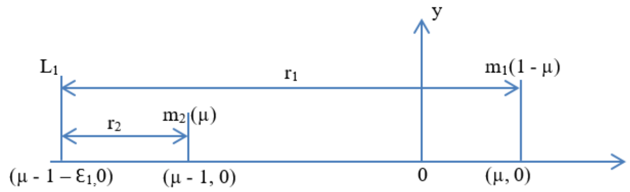

Figure 4. *Location of the collinear equilibrium point* L_1.

ε_1 is the distance between the smaller primary and L_1. Therefore,

$$x = \mu - 1 - \varepsilon_1.$$

$$r_1 = |x-\mu| = |\mu-1-\varepsilon_1-\mu+1| = |-(1+\varepsilon_1)| = 1+\varepsilon_1,$$

$$r_2 = |x-\mu+1| = |\mu-1-\varepsilon_1-\mu+1| = |-\varepsilon_1| = \varepsilon_1$$

Now substituting these values of x, r_1 and r_2 in eq. (14), and using $A_E = (1-\alpha_E)$, $A_M = (1-\alpha_M)$ it yields

$$n^2\beta(\mu-1-\varepsilon_1) + \frac{(1-\mu)(1-\alpha_E)}{(1+\varepsilon_1)^2} + \frac{3k_1(1-\alpha_E)}{2(1+\varepsilon_1)^4} + \frac{\mu(1-\alpha_M)}{\varepsilon_1^2} + \frac{3k_2(1-\alpha_M)}{2\varepsilon_1^4} - \frac{M_b(\mu-1-\varepsilon_1)}{\left((\mu-1-\varepsilon_1)^2+T^2\right)^{\frac{3}{2}}} = 0$$

Now multiply the above equation by $2\varepsilon_1^4(1+\varepsilon_1)^4\left((\mu-1-\varepsilon_1)^2+T^2\right)^{\frac{3}{2}}$,

it becomes,

$$\begin{aligned}&2n^2\beta(\mu-1-\varepsilon_1)\varepsilon_1^4(1+\varepsilon_1)^4\left((\mu-1-\varepsilon_1)^2+T^2\right)^{\frac{3}{2}}+2\alpha_E(1-\mu)\varepsilon_1^4(1+\varepsilon_1)^2\left((\mu-1-\varepsilon_1)^2+T^2\right)^{\frac{3}{2}}\\&+3k_1\alpha_E\varepsilon_1^4\left((\mu-1-\varepsilon_1)^2+T^2\right)^{\frac{3}{2}}+2\mu\alpha_M\varepsilon_1^2(1+\varepsilon_1)^4\left((\mu-1-\varepsilon_1)^2+T^2\right)^{\frac{3}{2}}\\&+3k_2\alpha_M(1+\varepsilon_1)^4\left((\mu-1-\varepsilon_1)^2+T^2\right)^{\frac{3}{2}}-2m_b\varepsilon_1^4(1+\varepsilon_1)^4(\mu-1-\varepsilon_1)=0\end{aligned} \tag{17}$$

Case 2: Location of $L_2\left(\mu-1<x<\mu\right)$

Let the collinear point L_2 be on the right side of the smaller primary at a distance ε_2 from it on the x-axis. Then

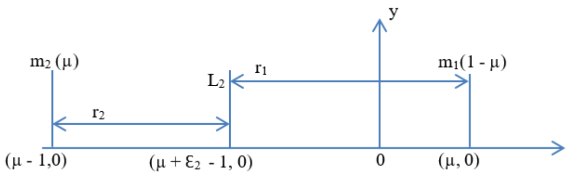

Figure 5. *Location of the collinear equilibrium point* L_2 ε_2 *is the distance between the smaller primary and* L_2.

Therefore,

$$x=\mu-1+\varepsilon_2\,,$$

$$r_1=\left|x-\mu\right|=\left|\mu-1+\varepsilon_2-\mu\right|=\left|-\left(1-\varepsilon_2\right)\right|=1-\varepsilon_2\,,$$

$$r_2=\left|x-\mu+1\right|=\left|\mu-1+\varepsilon_2-\mu+1\right|=\left|\varepsilon_2\right|=\varepsilon_2$$

Now substituting values of $r_1=1-\varepsilon_2$, $r_2=\varepsilon_2$ and $x=\mu-1+\varepsilon_2$ in eq. (4) and $A_E=\left(1-\alpha_E\right)$, $A_M=\left(1-\alpha_M\right)$ it yields

$$n^2\beta(\mu-1+\varepsilon_2)+\frac{(1-\mu)\alpha_E}{(1-\varepsilon_2)^2}+\frac{3k_1\alpha_E}{2(1-\varepsilon_2)^4}-\frac{\mu\alpha_M}{\varepsilon_2^2}-\frac{3k_2\alpha_M}{2\varepsilon_2^4}-\frac{M_b\left(\mu-1+\varepsilon_2\right)}{\left((\mu-1+\varepsilon_2)^2+T^2\right)^{\frac{3}{2}}}=0 \tag{18}$$

Now multiply the above equation by $2\varepsilon_2^4\left(1+\varepsilon_2\right)^4\left((\mu-1+\varepsilon_2)^2+T^2\right)^{\frac{3}{2}}$, it reduces to

$$\begin{aligned}&2n^2\beta(\mu-1+\varepsilon_2)\varepsilon_2^4(1-\varepsilon_2)^4\left((\mu-1+\varepsilon_2)^2+T^2\right)^{\frac{3}{2}}+2(1-\mu)\alpha_E\varepsilon_2^4(1-\varepsilon_2)^2\left((\mu-1+\varepsilon_2)^2+T^2\right)^{\frac{3}{2}}\\&+3k_1\alpha_E\varepsilon_2^4\left((\mu-1+\varepsilon_2)^2+T^2\right)^{\frac{3}{2}}-2\mu\alpha_M\varepsilon_2^2(1-\varepsilon_2)^4\left((\mu-1+\varepsilon_2)^2+T^2\right)^{\frac{3}{2}}\\&-3k_2\alpha_M(1-\varepsilon_2)^4\left((\mu-1+\varepsilon_2)^2+T^2\right)^{\frac{3}{2}}-2m_b(\mu-1+\varepsilon_2)\varepsilon_2^4(1-\varepsilon_2)^4=0\end{aligned} \tag{19}$$

Case 3: Location of $L_3\left(x<\mu\right)$

Let the collinear point L_3 be on the right side of the bigger primary at a distance ε_3 from it on the x-axis.

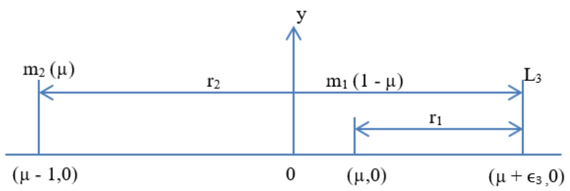

Figure 6. *Location of the collinear equilibrium point* L_3.

Then ε_3 is the distance between the bigger primary and L_3

Therefore,

$$x=\mu+\varepsilon_3\,,$$

Since $r_1=\left|x-\mu\right|=\left|\mu+\varepsilon_3-\mu\right|=\left|\varepsilon_3\right|=\varepsilon_3$,

$$r_2=\left|x-\mu+1\right|=\left|\mu+\varepsilon_3-\mu+1\right|=\left|1+\varepsilon_3\right|=1+\varepsilon_3$$

Now substituting the above values in eq. (15),

$A_E=\left(1-\alpha_E\right)$, $A_M=\left(1-\alpha_M\right)$ it yields

$$n^2\beta(\mu+\varepsilon_3)-\frac{(1-\mu)\alpha_E}{\varepsilon_3^2}-\frac{3k_1\alpha_E}{2\varepsilon_3^4}-\frac{\mu\alpha_M}{(1+\varepsilon_3)^2}-\frac{3k_2\alpha_M}{2(1+\varepsilon_3)^4}-\frac{M_b(\mu+\varepsilon_3)}{\left((\mu+\varepsilon_3)^2+T^2\right)^{\frac{3}{2}}}=0$$

Now multiply the above equation by $2\varepsilon_3^4(1+\varepsilon_3)^4\left((\mu+\varepsilon_3)^2+T^2\right)^{\frac{3}{2}}$, it yields;

$$\begin{aligned}&2n^2\beta(\mu+\varepsilon_3)\varepsilon_3^4(1+\varepsilon_3)^4\left((\mu+\varepsilon_3)^2+T^2\right)^{\frac{3}{2}}-2\alpha_E\varepsilon_3^2(1-\mu)(1+\varepsilon_3)^4\left((\mu+\varepsilon_3)^2+T^2\right)^{\frac{3}{2}}\\&-3k_1\alpha_E(1+\varepsilon_3)^4\left((\mu+\varepsilon_3)^2+T^2\right)^{\frac{3}{2}}-2\mu\alpha_M\varepsilon_3^4(1+\varepsilon_3)^2\left((\mu+\varepsilon_3)^2+T^2\right)^{\frac{3}{2}}\\&-3k_2\alpha_M\left((\mu+\varepsilon_3)^2+T^2\right)^{\frac{3}{2}}\varepsilon_3^4-2m_b(\mu+\varepsilon_3)\varepsilon_3^4(1+\varepsilon_3)^4=0\end{aligned}\tag{20}$$

4. Stability of Equilibrium Points

A study of the linear stability in the vicinity of any equilibrium point in the R3BP is performed by usually giving a small displacement with small velocity to the coordinate of the infinitesimal test particle. Then the equilibrium points is said to be stable for the oscillatory solutions with small amplitude and unstable, if a rapid departure of the test particle is occurred from the equilibrium point.

Let the location of an equilibrium point be donated by (a_0,b_0) and consider a small displacement (ξ,η) from the point such that the location becomes $(a_0+\xi),(b_0+\eta)$ consequently, the variational equations of motion are

$$\begin{aligned}\ddot{\xi}-2n\alpha\dot{\eta}&=\Omega_{xx}^0\xi+\Omega_{xy}^0\eta\\ \ddot{\eta}+2n\alpha\dot{\xi}&=\Omega_{xy}^0\xi+\Omega_{yy}^0\eta\end{aligned}\tag{21}$$

And the corresponding characteristic equation is

$$\lambda^4-\left(\Omega_{xx}^0+\Omega_{yy}^0-4\alpha^2n^2\right)\lambda^2+\Omega_{xx}^0\Omega_{yy}^0-\left(\Omega_{xy}^0\right)^2=0\tag{22}$$

Where

$\Omega_{xx}^0,\Omega_{yy}^0,\Omega_{xy}^0$ are second order partial derivatives which will be evaluated at the equilibrium point under consideration

4.1. Triangular Points

The stability of the triangular point is determined by the nature of the roots of the eq. (22). The second order partial derivatives can be written with the help of equation (4).

$$\begin{aligned}\Omega_{xx}=&\,n^2\beta-\frac{(1-\mu)A_E}{r_1^3}+\frac{3(1-\mu)A_E(x-\mu)^2}{r_1^5}-\frac{3k_1A_E}{2r_1^5}+\frac{15(x-\mu)^2k_1A_E}{2r_1^7}-\frac{\mu A_M}{r_2^3}+\frac{3\mu(x-\mu+1)^2A_M}{r_2^5}-\frac{3k_2A_M}{2r_2^5}\\&+\frac{15(x-\mu+1)^2k_2A_M}{2r_2^7}-\frac{M_b}{\left(r^2+T^2\right)^{\frac{3}{2}}}+\frac{3M_bx^2}{\left(r^2+T^2\right)^{\frac{5}{2}}}\end{aligned}$$

$$\begin{aligned}\Omega_{yy}=&\,n^2\beta-\frac{(1-\mu)A_E}{r_1^3}+\frac{3(1-\mu)A_Ey^2}{r_1^5}-\frac{3k_1A_E}{2r_1^5}-\frac{\mu A_M}{r_2^3}+\frac{15k_1A_Ey^2}{2r_1^7}-\frac{3k_2A_M}{2r_2^5}\\&+\frac{15k_2A_My^2}{2r_2^7}+\frac{3\mu A_My^2}{r_2^5}-\frac{M_b}{\left(r^2+T^2\right)^{\frac{3}{2}}}+\frac{3M_by^2}{\left(r^2+T^2\right)^{\frac{5}{2}}}.\end{aligned}$$

$$\Omega_{xy} = \frac{3(1-\mu)A_E(x-\mu)\ y}{r_1^5} + \frac{15(x-\mu)\ k_1 A_E y}{2r_1^7} + \frac{3\mu y(x-\mu+1)\ A_m}{r_2^5} + \frac{15(x-\mu+1)k_2 A_m y}{2r_2^7} + \\ + \frac{3M_b x\ y}{\left(r^2+T^2\right)^{\frac{5}{2}}} \tag{23}$$

These second order partial derivatives are computed at the triangular points obtained in eq. (13) retaining only linear terms as;

$$\Omega_{xx}^0 = \frac{3}{4} + \frac{5}{4}\varepsilon' - \frac{2}{3}(1-3\mu)\alpha_E + \frac{2}{3}(2-3\mu)\alpha_m + \frac{3(1-2\mu)}{2(1-\mu)}k_1 - \frac{3(1-2\mu)}{2\mu}k_2 + \frac{15k_3}{8} + \frac{5M_b(2r_c-1)}{4(r_c^2+T^2)^{\frac{3}{2}}} + \frac{3M_b}{4(r_c^2+T^2)^{\frac{5}{2}}}$$

$$\Omega_{yy}^0 = \frac{9}{4} + \frac{7\in'}{4} + \frac{1}{2}(1-3\mu)\alpha_E - \frac{1}{2}(2-3\mu)\alpha_m + \frac{3k_1}{2(1-\mu)} + \frac{3k_2}{2\mu} + \frac{21k_3}{8} \\ + \frac{7}{4}\frac{M_b(2r_c-1)}{\left(r_c^2+T^2\right)^{\frac{3}{2}}} + \frac{9M_b}{4\left(r_c^2+T^2\right)^{\frac{5}{2}}}$$

$$\Omega_{xy}^0 = \sqrt{3}\left[-\frac{3}{4} + \frac{3\mu}{2} - \left(\frac{1}{6}+\frac{1}{6}\mu\right)\alpha_E - \left(\frac{1}{3}-\frac{1}{6}\mu\right)\alpha_m - \frac{11\in'}{12} - \frac{(2-\mu)}{2(1-\mu)}k_1 + \frac{(1+\mu)}{2\mu}k_2 + \frac{11(2\mu-1)k_3}{8} \right. \\ \left. -\left\langle\frac{11}{12} - \frac{11\mu}{6}\right\rangle\frac{M_b(2r_c-1)}{\left(r_c^2+T^2\right)^{\frac{3}{2}}} - \frac{3M_b\left(\frac{1}{2}-\mu\right)}{2\left(r_c^2+T^2\right)^{\frac{5}{2}}} + \frac{11\mu\in'}{6}\right] \tag{24}$$

Now, substituting eq. (24), in to the characteristic equation (22) and simplifying, we get

$$\lambda^4 + h_1\lambda^2 + h_2 = 0 \tag{25}$$

where

$$h_1 = 4n^2\alpha^2 - \left(\Omega_{xx}^0 + \Omega_{yy}^0\right) = 1 + 8\varepsilon - 3\varepsilon' - 3(k_1+k_2) + \frac{3k_3}{2} + \frac{M_b(2r_c+3)}{\left(r_c^2+T^2\right)^{\frac{3}{2}}} - \frac{M_b 3r_c^2}{\left(r_c^2+T^2\right)^{\frac{5}{2}}}$$

$$h_2 = \Omega_{xx}^0\Omega_{yy}^0 - \left(\Omega^0{}_{xy}\right)^2 = \frac{27\mu}{4} - \frac{27\mu^2}{4} + \frac{33\mu\varepsilon'}{2} - \frac{33\mu^2\varepsilon'}{2} + \frac{3\mu}{2}(\alpha_E+\alpha_M) - \frac{3\mu^2}{2}(\alpha_E+\alpha_M) + \frac{9\mu}{2}(k_1-k_2) \\ + \frac{9k_2}{2} + \frac{99k_3}{4}\left(\mu-\mu^2\right) + \frac{33\mu(1-\mu)\left(2r_c^2-1\right)M_b}{2\left(r_c^2+T^2\right)^{\frac{3}{2}}} + \frac{27\mu(1-\mu)M_b}{4\left(r_c^2+T^2\right)^{\frac{5}{2}}}$$

Its roots are

$$\lambda^2 = \frac{-h_1 \pm \sqrt{\Delta}}{2} \tag{26}$$

where

$$\Delta = h_1^2 - 4h_2 \tag{27}$$

can be simplified by considering the linear terms of small quantities only to

$$\Delta = \left(27 + 66\in' + 6\alpha_E + 6\alpha_m + 99k_3 + \frac{66M_b(2r_c - 1)}{(r_c^2 + T^2)^{\frac{3}{2}}} + \frac{27M_b}{(r_c^2 + T^2)^{\frac{5}{2}}}\right)\mu^2 + \left(-27 - 66\in' - 6\alpha_E - 6\alpha_m - 18k_1 + 18k_2 - 99k_3 - \frac{66M_b(2r_c - 1)}{(r_c^2 + T^2)^{\frac{3}{2}}} + \frac{27M_b}{(r_c^2 + T^2)^{\frac{5}{2}}}\right)\mu + 1 + 16\varepsilon - 6\in' - 6(k_1 + k_2) + 3k_3 - 18k_2 + \frac{2M_b(2r_c + 3)}{(r_c^2 + T^2)^{\frac{3}{2}}} - \frac{6M_b r_c^2}{(r_c^2 + T^2)^{\frac{5}{2}}} \tag{28}$$

The critical mass ratio μ_c is a value of $\mu\left(0 < \mu < \frac{1}{2}\right)$ for which $\Delta = 0$. Therefore

$$\mu_c = \mu_0 + \mu_h + \mu_a + \mu_p + \mu_b \tag{29}$$

With

$$\mu_0 = \frac{1}{2}\left(1 - \sqrt{\frac{23}{27}}\right),$$

$$\mu_h = -\frac{1}{3}\left[\left(1 + \frac{15}{\sqrt{69}}\right)k_2 - \left(1 - \frac{15}{\sqrt{69}}\right)k_1\right] - \frac{2}{9\sqrt{69}}k_3,$$

$$\mu_a = -\frac{2\alpha_E}{27\sqrt{69}} - \frac{2\alpha_m}{27\sqrt{69}}$$

$$\mu_p = \frac{4(36\varepsilon - 19\varepsilon')}{27\sqrt{69}}$$

$$\mu_b = \frac{\left[4(19 - 2r_c)(r_c^2 + T^2)^{\frac{5}{2}} - 9(1 + 6r_c^2)(r_c^2 + T^2)^{\frac{3}{2}}\right]M_b}{27\sqrt{69}(r_c^2 + T^2)^4}$$

The first term μ_0 represents Routh's critical mass value; the second term μ_h is the effect arising from heterogeneity of both primaries, the third term μ_α denotes the effect of the Albedo; the fourth term μ_p is the measure of the impact of small perturbations in the Coriolis and centrifugal forces; the last one is due to the gravitational potential from the circumbinary disc (belt). Clearly equation (29) is a combined effect of the participating parameters.

4.2. Collinear Points

The partial derivatives computed (24) at any collinear point $(x_0, 0)$, are

$$\Omega_{xx}^0 = n^2\beta + \frac{2(1-\alpha_E)(1-\mu)}{|x_0 - \mu|^3} + \frac{6k_1(1-\alpha_E)}{|x_0 - \mu|^5} + \frac{2\mu(1-\alpha_M)}{|x_0 - \mu + 1|^3} + \frac{6k_2(1-\alpha_M)}{|x_0 - \mu + 1|^5} + \frac{3M_b x_0^2}{(x_0^2 + T^2)^{\frac{5}{2}}} - \frac{M_b}{(x_0^2 + T^2)^{\frac{3}{2}}} > 0,$$

$$\Omega_{yy}^{0}=n^{2}\beta-\frac{(1-\mu)(1-\alpha_{E})}{\left|x_{0}-\mu\right|^{3}}-\frac{3k_{1}(1-\alpha_{E})}{2\left|x_{0}-\mu\right|^{5}}-\frac{\mu(1-\alpha_{M})}{\left|x_{0}-\mu+1\right|^{3}}-\frac{3k_{2}(1-\alpha_{M})}{2\left|x_{0}-\mu+1\right|^{5}}-\frac{M_{b}}{(x_{0}^{2}+T^{2})^{\frac{3}{2}}}<0$$

$$\Omega_{xy}^{0}=\Omega_{yx}^{0}=0 \tag{30}$$

Substitution of these values in the characteristic equation (22) reduces to:

$$\lambda^{4}+\left(4n^{2}\alpha^{2}-(\Omega_{xx}^{0}+\Omega_{yy}^{0})\right)\lambda^{2}+\Omega_{xx}^{0}\Omega_{yy}^{0}=0 \tag{31}$$

The equilibrium point is stable if all the roots of the characteristic equation are either negat ive real numbers or distinct pure imaginary numbers or the complex numbers with negative real part eqs. (33) to (34) show that the collinear points lying in the intervals with respect to their primaries, given that

$$\Omega_{xx}^{0}>0.$$

$$\Omega_{yy}^{0}<0,\quad \Omega_{yx}^{0}=\Omega_{xy}^{0}=0.$$

Therefore,

$\Omega^{0}{}_{xx}\Omega^{0}{}_{yy}<0$, and the determinant of eq. (31) is positive.

This means that the two roots of the characteristic equation (31) are real numbers but opposite in sign and the other roots are purely imaginary numbers in the conjugate pairs. Therefore, the roots can be expressed as $\lambda_{1,2}=\pm a$ and $\lambda_{3,4}=\pm ib$ where a and b are real. This implies that the motion in the neighbourhood of the collinear points is not bounded and unstable.

5. Numerical Application for the Earth-Moon System

Table 1. *Effects of the parameters involved on the positions of the triangular equilibrium points and their critical mass for the Earth-Moon system.* $(\mu=0.01215)$.

Case	K₁	K₂	K₃	ε	ε'	M_b	α_E	x	$\pm y$	μ_c	Remark
1.	0	0	0	0	0	0	1	-0.48785	0.86603	0.03852	Stable
2.	1.58303×10^{-7}	9.83933×10^{-18}	3.13153×10^{-8}	0.001	0.003	0.02	0.040	-0.63712	0.75639	0.03389	Stable
3.	1.58303×10^{-7}	0	3.13153×10^{-8}	0	0	0	0	0.48785	0.86603	0.03852	Stable
4.	1.58303×10^{-7}	9.83933×10^{-18}	3.13153×10^{-8}	0.001	0.003	0	0	0.48785	0.86604	0.03815	Stable
5.	0	0	0	0.001	0.003	0.02	0	0.48785	0.85797	0.03860	Stable
6.	1.58303×10^{-7}	9.83933×10^{-18}	3.13153×10^{-8}	0	0	0	0.040	-0.63719	0.75677	0.03426	Stable
7.	0	0	0	0.001	0.003	0.02	0.040	-0.63713	0.75638	0.03389	Stable
8.	0	0	0	0	0	0.02	0.040	-0.63713	0.75677	0.03426	Stable
9.	0	9.83933×10^{-18}	0	0	0	0.02	0.040	-0.63713	0.75677	0.03426	Stable

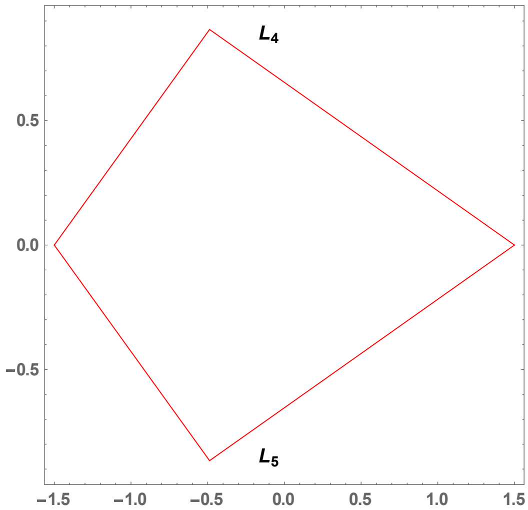

Figure 7. *Triangular points in the classical case of the Earth-Moon system.*

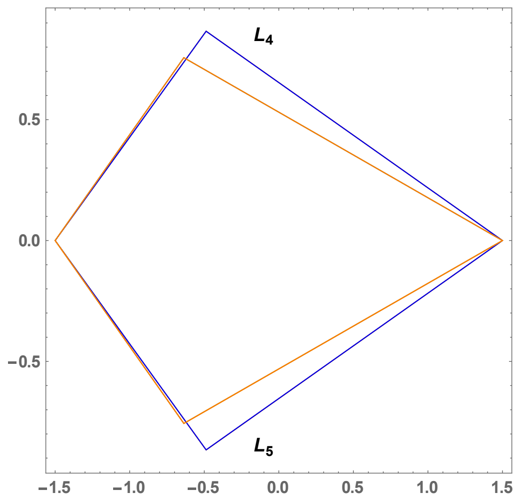

Figure 8. *Combined effects of perturbations, Albedo, Heterogeneity of the primaries and circumbinary disc on the triangular points for the Earth-Moon system.*

The graphs below show the effects of various parameters on the Critical Mass Value (μ_c) for the Earth-Moon system.

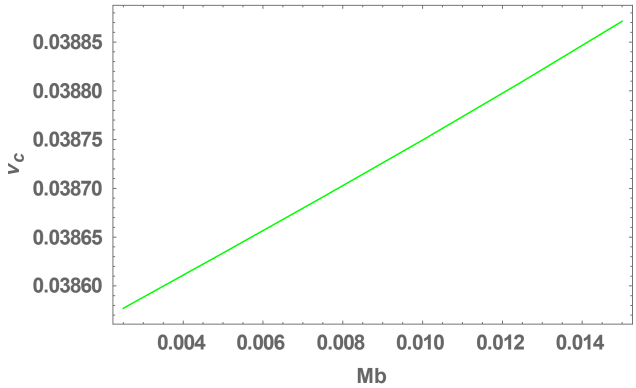

Figure 9. *Effect of the potential from the belt on the critical mass ratio.*

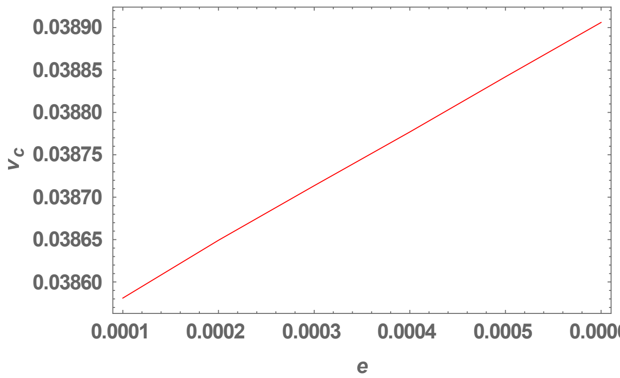

Figure 10. *Effect of the small perturbation on the critical mass ratio μ_c this shows that the increase of the perturbation leads to the increase of the critical mass ratio.*

Table 2. *Effects of various parameter on the positions of collinear libration points* $L_{1,2,3}, L_{n3}$ $(\mu = 0.1215)$ *for the Earth-Moon system.*

Cases	k_1	k_2	k_3	β	α_E	M_b	L_1	L_2	L_3	L_{n3}
1	0	0	0	1.00	1	0	−1.2958	-0.1468	0.8666	0.147
2	1.5830×10^{-7}	9.839×10^{-18}	3.13153×10^{-8}	1.001	4.7×10^{-15}	0.02	−1.2958	-0..0594	0.6306	-
3	1.5830×10^{-7}	9.8393×10^{-18}	3.13153×10^{-8}	1.00	0	0	−1.1557	-0.3321	0.6680	-
4	1.5830×10^{-7}	9.8393×10^{-18}	3.13153×10^{-8}	1.00	4.7×10^{-15}	0.0	−1.0916	-0.3219	0.6781	
5	1.5830×10^{-7}	9.83933×10^{-18}	3.13153×10^{-8}	1.00	4.7×10^{-15}	0.025	−1.0916	-0.4601	0.3255	1.005 1.5185

Cases	k_1	k_2	k_3	β	α_E	M_b	L_1	L_2	L_3	L_{n3}
6	0	0	0	1.0004	4.7×10^{-15}	0.027	-1.2439	-0.4086	0.5123	1.0005 1.4085
7	0	0	0	1.0005	0	0.0025	-1.2766	-0.1378	0.3450	1.5089

The effects of the parameters on the positions of the collinear points are shown in Table 3 numerically and in Figures 11 to 15 graphically for the Earth-Moon system.

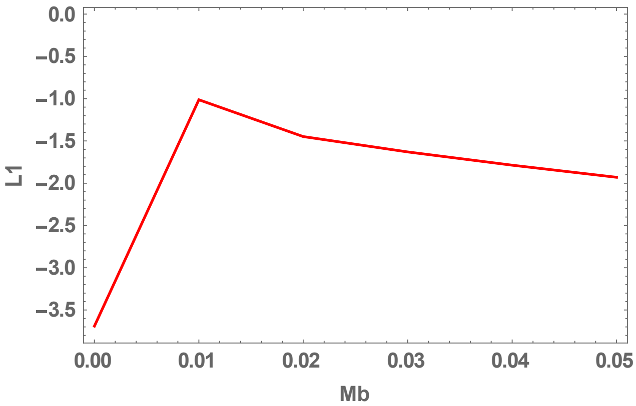

***Figure 11**. Effect of the potential due to belt on the collinear point L_1. This shows that the point L_1 shift away from the origin with increase in potential.*

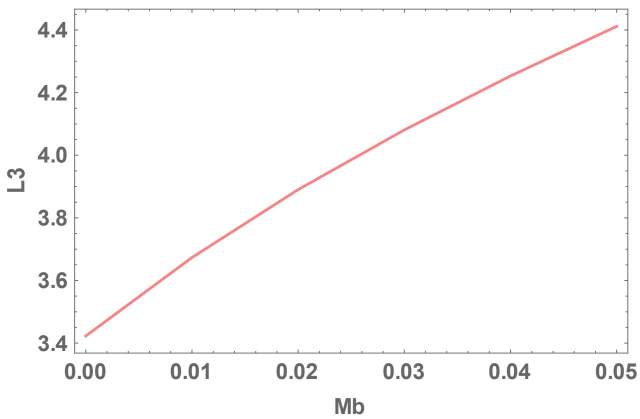

***Figure 13**. Effect of the Belt on the collinear point on L_3.*

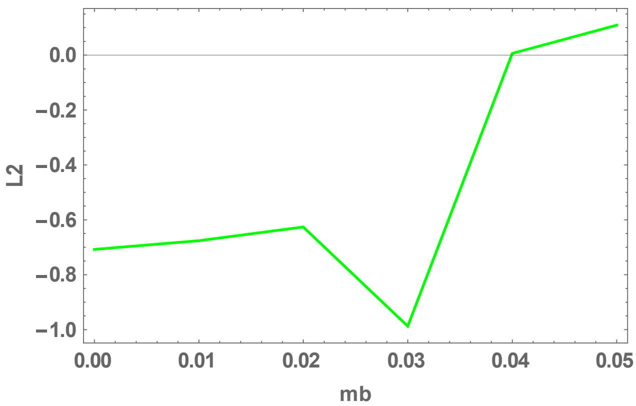

***Figure 12**. Effect of the potential from the belt on the collinear point L_2 which shows that due to the increase of potential from the belt the point shift away from the origin.*

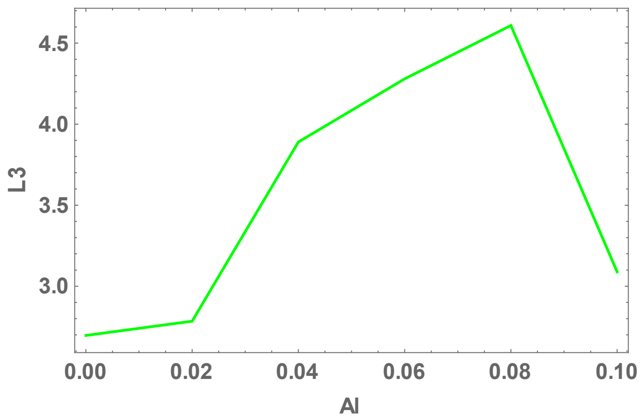

***Figure 14**. Effect of the Albedo on the collinear point L_3.*

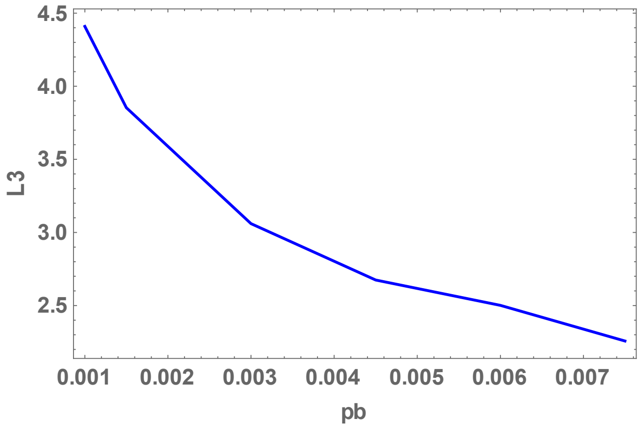

Figure 15. *Effect of the small perturbation of the centrifugal force on the collinear point L_3.*

Table 3. *The characteristic roots* $(\lambda_{1,2};\ \lambda_{3,4})$ *of collinear point* $(L_1.)$ *for the Earth-Moon system:* $\mu = 0.01215, T = 0.01$.

Cases	k_1	k_2	k_3	β	α_E	M_b	L_1	$\lambda_{1,2}$	$\lambda_{3,4}$	Remark
1	0	0	0	1.00	1	0	-1.2958	±46.6262	±1.2815i	Unstable
2	1.58302×10^{-7}	9.83933×10^{-18}	3.13153×10^{-8}	1.001	4.7×10^{-15}	0.02	-1.0868	±4.2481	±2.6333i	Unstable
3	1.58302×10^{-7}	9.83933×10^{-18}	3.13153×10^{-8}	1.0000	0	0	-1.1557	±2.8785	±1.3697i	Unstable
4	1.58302×10^{-7}	9.83933×10^{-18}	3.13153×10^{-8}	1.0000	4.7×10^{-15}	0.00	0.00	±2.8226	±1.6165i	Unstable
5	1.58302×10^{-7}	9.83933×10^{-18}	3.13153×10^{-8}	1.0000	4.7×10^{-15}	0.026	-1.0916	±4.0062	±2.4354i	Unstable
6	0	0	0	1.0005	4.7×10^{-15}	0.027	-1.2439	±54.9677	±22.0116i	Unstable
7	0	0	0	1.00	1	0.025	-1.2766	±54.7606	±1.3612i	Unstable

Table 4. *The characteristic roots* $(\lambda_{1,2};\ \lambda_{3,4})$ *of collinear point* $(\ L_2\ )$ *for the Earth-Moon system:* $\mu = 0.01215, T = 0.01$.

Cases	k_1	k_2	k_3	β	α_E	M_b	L_1	$\lambda_{1,2}$	$\lambda_{3,4}$	Remark
1	0.00	0.00	0.00	1.00	1	0.00	-0.1468	±24.3133	±15.6121i	Unstable
2	1.58302×10^{-7}	9.83933×10^{-18}	3.13153×10^{-8}	1.001	4.7×10^{-15}	0.02	-0.5094	±4.1228	±2.5270i	Unstable
3	1.58302×10^{-7}	9.83933×10^{-18}	3.13153×10^{-8}	1.0000	0	0.00	-0.3321	±7.0382	±4.8237i	Unstable
4	1.58302×10^{-7}	9.83933×10^{-18}	3.13153×10^{-8}	1.0000	4.7×10^{-15}	0.00	-0.3219	±7.1615	±4.9270i	Unstable
5	1.58302×10^{-7}	9.83933×10^{-18}	3.13153×10^{-8}	1.0000	4.7×10^{-15}	0.026	-0.4601	±4.0234	±2.4457i	Unstable
6	0.00	0.00	0.00	1.0005	4.7×10^{-15}	0.027	-0.4086	±24.8244	±3.5154i	Unstable
7	0.00	0.00	0.00	1.0006	1	0.025	-0.1378	±28.2630	±17.0436i	Unstable

Table 5. *The characteristic roots* $(\lambda_{1,2};\ \lambda_{3,4})$ *of collinear point* (L_3) *for the Earth-Moon system:* $\mu = 0.1215, T = 0.01$.

Cases	k_1	k_2	k_3	β	α_E	M_b	L_1	$\lambda_{1,2}$	$\lambda_{3,4}$	Remark
1	0	0	0	1.00	1	0.02	0.8666	± 4.3760	$\pm 0.9555i$	Unstable
2	1.58302×10^{-7}	9.83933×10^{-18}	3.13153×10^{-8}	1.001	4.7×10^{-15}	0	0.6306	± 3.1063	$\pm 1.6447i$	Unstable
3	1.58302×10^{-7}	9.83933×10^{-18}	3.13153×10^{-8}	1.0000	0	0	0.6680	± 2.8302	$\pm 1.5827i$	Unstable
4	1.58302×10^{-7}	9.83933×10^{-18}	3.13153×10^{-8}	1.0000	4.7×10^{-15}	0.026	0.6781	± 2.6844	$\pm 1.4920i$	Unstable
5	1.58302×10^{-7}	9.83933×10^{-18}	3.13153×10^{-8}	1.0000	4.7×10^{-15}	0.027	0.3255	± 7.9223	$\pm 5.4111i$	Unstable
6	0	0	0	1.0005	4.7×10^{-15}	0.025	0.5123	± 14.1690	$\pm 2.1829i$	Unstable
7	0	0	0	1.0006	1	0.02	0.3450	± 37.6851	$\pm 4.7764i$	Unstable

Table 6. *The characteristic roots* $(\lambda_{1,2};\ \lambda_{3,4})$ *of collinear point* (L_{n3}) *for the Earth-Moon system:* $\mu = 0.1215, T = 0.01$.

Cases	k_1	k_2	k_3	β	α_E	M_b	L_1	$\lambda_{1,2}$	$\lambda_{3,4}$	Remark
5	1.58302×10^{-7}	9.83933×10^{-18}	3.13153×10^{-8}	1.0000	4.7×10^{-15}	0.026	1.5185 1.0005	± 1.3822 ± 1.8916	$\pm 1.1565i$ $\pm 1.8916i$	Unstable Unstable
6	0.00	0.00	0.00	1.0005	4.7×10^{-15}	0.027	1.0005 1.4085	± 3.3330 ± 2.1043	$\pm 1.3769i$ $\pm 1.7040i$	Unstable Unstable
7	0.00	0.00	0.00	1.0006	0	0.025	1.5089	± 2.2032	$\pm 1.5886i$	Unstable

6. Discussion

The modified equations (1) described the motion of the third body under the combined influence of Albedo and heterogeneity of the primaries, small perturbations and potential from a belt. The locations of triangular points are obtained in equation (13) analytically. It is found that they form triangles with the line joining the primaries. Clearly, the positions of triangular points are characterized by the all participating parameters. With the help of software MATHEMATICA, the ZVCs for the Earth-Moon system are shown in different cases using equation (3) at a given Jacobian constant C. The figures are demonstrated for the curved in (2-D) and its correspondence in (3-D) respectively. The circular regions are allow the infinitesimal body to motion while the smaller cyclic region near the smaller primary are not allow to move. The effects of the parameters involved eq. (13) on the locations of triangular points and critical mass ratio for the Earth-Moon system are presented in the Table 1, numerically and in Figures 7 to 8 graphically, it shows how the positions of the triangular points are influenced by the aforementioned parameters. It is observed that, the triangular points do not form equilateral triangles as they do in the classical.

The graphs shown in Figures 9 and 10, is the effects of various parameters on the Critical Mass Value (μ_c) where it was influenced by the effects of Albedo, heterogeneity of the primaries; small perturbations and the potential from a belt. We have observed the Coriolis force and the belt possess stabilizing tendency, while the centrifugal force, Albedo effect and heterogeneity of the primaries have destabilizing behaviour.

Using the software MATHEMATICA, the numerical values are computed using equations (17), (19) and (20) in order to obtain the collinear equilibrium positions. These values are tabulated which corresponding to collinear positions $(L_1, L_2\ L_3\ and\ L_{n3})$ for the Earth-Moon system respectively. We observed that in each of the positions shown in Table 2, effects of various perturbations considered as the participated parameters, albedo, the potential due to Belt and the heterogeneity of the primaries. Tables 3, 4, 5, and 6 indicate the stability of the collinear equilibrium points, the region of stability of the collinear positions decreases for the Earth-Moon system. The collinear of this case still remain unstable as in the proceeded researchers.

In the case when heterogeneity and albedo of the primaries are ignore, the results presented here are in agreement with those of Singh and Taura (15), if its oblateness are absent. In the absence of both heterogeneity of the primaries, the potential from a belt and albedo, our results obtained are in agreement with those of Singh and Haruna (13), if its bodies are spherical with presence of radiation pressure. In the absence of drag force, perturbations and heterogeneity of the primaries and albedo, while the primaries are luminous and there is effect of potential from a belt, our results coincide with those obtained by Singh and Amuda [18]. Many results can be validated from our findings.

The equilibrium points have various applications in astronomy, space exploration, and celestial mechanics. These applications extend to:

1) Spacecraft Positioning and Observation:

Space agencies place satellites at Lagrangian points for long-term observations because of their gravitational stability.

Examples:

The *James Webb Space Telescope (JWST)* is located at *L2* (Earth-Sun system) for deep space observation.

The *Solar and Heliospheric Observatory (SOHO)* is positioned at *L1* for continuous monitoring of the Sun.

2) Communication Satellites:

Communication satellites are often placed at equilibrium points in the Earth-Moon system for stable relay stations between Earth and distant spacecraft.

Fuel-Efficient Space Missions:

Equilibrium points are used in mission planning to reduce fuel consumption by allowing spacecraft to "hover" using minimal propulsion.

7. Conclusion

This paper has determined the positions of triangular points and their linear stability when both primaries are heterogeneous oblate spheroids associated with albedo effect and surrounded by a circumbinary disc under the influence effects of perturbed Coriolis and centrifugal forces. It is discovered that positions are not affected by a small perturbation given to the Coriolis force. The stability of motion is found only in $0 < \mu < \mu_c$, where μ_c is influenced by the effects of albedo, heterogeneity of the primaries, small perturbations, and the potential from a belt. We have observed that the Coriolis force and the belt possess stabilizing tendency, while the centrifugal force, albedo and heterogeneity of the primaries have destabilising behaviour. The instability of the collinear points remains unchanged, as in the classical case, even with the additional new collinear point. This is confirmed by numerical analysis, which reveals the existence of at least one positive root. The motion of the infinitesimal body is unbounded, and the collinear libration points are unstable. Although this paper has generalized all the problems of the R3BP when the shape, radiation, albedo, heterogeneity behaviour of the participating bodies and small perturbations in the Coriolis and centrifugal forces couple with belt are considered; nevertheless, we can still find an extension of the problem. These may include the followings.

a) A study when the P-R (Poynting-Robertson) drag forces are considered.
b) Work of variable mass problem may be carried out.
c) The case when the primaries move in an elliptical orbits.
d) An inclusion of triaxial primaries couple with Potential from a belt.
e) CRTBP with Yukawa-like corrections to Newtonian potential under a radiation primary model.
f) CRTBP with Yukawa-like corrections to Newtonian potential under perturbations with heterogeneous oblate spheroid primaries and potential from a belt model.
g) Equilibrium points in CRTBP with Yukawa-like corrections to Newtonian potential under a triaxial primary model.
h) Non-collinear equilibrium points in ERTBP with Yukawa-like corrections to Newtonian potential.

Abbreviations

Q	Radiation Factor (Mass Reduction Factor)
M	Mass Ratio
μ_c	Critical Mass Ratio
r_1	Distance of Infinitesimal Mass from the Bigger Primary
r_2	Distance of Infinitesimal Mass from the Smaller Primary
Ω	Force Function
G	Gravitational Constant
F_g	Gravitational Force of Attraction
M	Infinitesimal Mass
N	Mean Motion
A	Oblateness Coefficient
$L_{1,2,3}$	Collinear Equilibrium Points
$L_{4,5}$	Triangular Equilibrium Points
F_p	Radiation Pressure Force
$k_i (i = 1, 2, 3)$	Parameters for Being Heterogeneous Primaries with Three Layers of Different Densities
$q_i (i = 1, 2)$,	Radiation Factors of the Primary and the Secondary
$\alpha = 1 + \varepsilon, \varepsilon << 1$	Parameters for the Coriolis, Which Small Perturbation ε is Given
$\beta = 1 + \varepsilon'$, $\varepsilon' << 1$	Parameters for the Centrifugal Force to Which Small Perturbation ε' is Given
M_b	Total Mass of the Belt (Circular Cluster of Material Points)
r	Radial Distance of the Infinitesimal Body

r_c	The Classical Case
$T = a + b$; a and b	Parameters Which Determine the Density Profile of the Belt
a	Parameter That Controls the Flatness of the Profile and is Known as the Flatness Parameter
b	Parameter Controls the Size of the Core of the Density Profile and is Called the Core Parameter
A_E	Albedo Factor of the Bigger Primary, s $1-\propto_E$
A_M	Albedo Factor of the Smaller Primary, $1-\propto_M$
l_1	Luminosity of the Bigger
l_2	Luminosity of the Smaller Primary
c	Speed of Light
σ	Mass per Unit Area of the Infinitesimal Mass

Conflicts of Interest

The authors declare no conflicts of interest.

References

[1] AbdulRaheem, A. and Singh, J. (2006). Combined effects of perturbations, radiation and oblateness on the stability of libration points in the restricted three-body problem. *Astronomical journal,* 131: 1880-1885. https://doi.org/10.1086/500654

[2] Ansari, A. A., Alhussain, Z. A and Prassad, S. N. (2018). ER3BP when the smaller Primaries are heterogeneous Spheroid of three layers and infinitesimal body varies its mass. *J. Astrophys. Astron.* 39, 57. https://doi.org/10.1007/s12036-018-9540-7

[3] Idrisi, M. J. (2017). A study of libration points in CR3BP under albedo effect. *International Journal of Advanced Astronomy*, 5: 1-6.

[4] Idrisi, M. J. (2017a). A Study of Libration Points in Modified CR3BP Under Albedo Effect when Smaller Primary is an Ellipsoid. *Journal of the Astronautical Sciences*, 64: 379-398. https://doi.org/10.1007/s40295-017-0115-7

[5] Idrisi, M. J. and Ullah, M. S. (2018). Non-collinear libration points in ER3BP with albedo effect and oblateness. *Journal of Astrophysics and Astronomy*, 39: 1-10. https://doi.org/10.1007/s12036-018-9520-y

[6] Idrisi, M. J. and Ullah, M. S. (2020). A Study of Albedo Effects on Libration Points in the Elliptic Restricted Three-Body Problem. *Journal of the Astronautical Sciences*, 67: 863-879.

[7] Jiang, I. G and Yeh, L. C.(2006). On the chermnyks-like, The equilibrium points. *Astrophs. space sci. 306, 189-200* https://doi.org/10.1007/s10509-006-9186-9

[8] Kumari Shalini. M. Javed Idrisi. J. K. Singh. M. Shahbaz ullah (2023). Stability analysis in the R3BP under the effect of heterogeneous Spheroid. *New Astronomy.* (2023).104, 102556. https://doi.org/10.1016/j.newast.2023.102556

[9] Kumari Shalini. Md sanam Suraj. Rajiv Aggarwal (2016). The Nonlinear stability of L_4 in the R3BP when the smaller Primary is a heterogeneous Spheroid. *American Astronautical society.* 64, 18: 49 (2016). https://doi.org/10.1007/s40295-016-0093-1

[10] Md sanam Suraj. M. R. Hassan. Md chan Asique (2014). The Photo gravitational R3BP when the Primaries are Heterogeneous Spheroid with Three Layers. *American Astronautical society.* 61, 133 (2014). https://doi.org/10.1007/s40295-014-0026-9

[11] Shipra Chauhan, Denish Kumar and Bhavneet Kaur (2018). Restricted Three body problem under the effect of Albedo, when the smaller primary is a finite straight segment. *Appl. math*. ISSN: 1932-9466, vol. 13, 2 (2018), pp: 1200-1215.

[12] Singh, J. and Haruna (2014). Equilibrium Points and stabilty under effect of Radiation, perturbating forces in the Restricted Problem of Three oblate bodies. *Astrophysics and Space Science,* 349, 107-115. https://doi.org/10.1007/s10509-013-1627-7

[13] Singh, J. and Haruna (2020). Motion around the Triangular Equilibrium Points in the Circular Restricted Three-Body Problem with radiating heterogeneous primaries surrounde by a belt. *Scientific report* (2020). 18861. https://doi.org/10.1038/s41598-020-75174-7

[14] Singh, J. and Taura, J. J. (2013). Motion in the generalized restricted three-body problem" *Astrophysics and Space Science,* 343: 95-106. https://doi.org/10.1007/s10509-012-1225-0

[15] Singh, J. and Taura, J. J. (2014). Effect of Triaxial, oblateness and Gravitational potential from the belt on the linear stability of $L_{4,5}$ in the R3BP. *Astrophysics and Space Science,* 35: 729-743. https://doi.org/10.1007/s12036-014-9308-7

[16] Singh, J. and Tyokyaa, K. R. (2023). Albedo effects in the ER3BP with an oblate primary, a triaxial secondary and a potential due to belt. *Scientific reports,* (2023) 13: 4286. https://doi.org/10.1038/s41598-023-30671-3

[17] Singh, J., and Ishwar, B. (1999). Stability of triangular points in the generalized photo gravitational restricted three body problem. *Aryabhatta Research Institute of Observatory Science. India,* 27: 415-424.

[18] Singh, J. and Amuda T. O (2019). Stability analysis of triangular equilibrium points in the restricted three-body problem under effects of circumbinary disc, radiation and drag forces. *Journal of Astrophysics and Astronomy* 40, 5. https://doi.org/10.1007/s12036-019-9573-6

[19] Singh, J. and Taura, J. J (2016). Combined effects of oblateness, radiation and cluster of material points on the stability of triangular libration points in R3BP. *Astrophysics and space science.* https://doi.org/10.1007/s10509-014-1860-8